Rapid Communications

Transverse spin transfer to Λ and $\bar{\Lambda}$ hyperons in polarized proton-proton collisions at $\sqrt{s} = 200$ GeV

J. Adam,[12] L. Adamczyk,[2] J. R. Adams,[35] J. K. Adkins,[26] G. Agakishiev,[24] M. M. Aggarwal,[37] Z. Ahammed,[57] I. Alekseev,[3,31] D. M. Anderson,[51] R. Aoyama,[54] A. Aparin,[24] D. Arkhipkin,[5] E. C. Aschenauer,[5] M. U. Ashraf,[53] F. Atetalla,[25] A. Attri,[37] G. S. Averichev,[24] X. Bai,[10] V. Bairathi,[32] K. Barish,[9] A. J. Bassill,[9] A. Behera,[49] R. Bellwied,[19] A. Bhasin,[23] A. K. Bhati,[37] J. Bielcik,[13] J. Bielcikova,[34] L. C. Bland,[5] I. G. Bordyuzhin,[3] J. D. Brandenburg,[42] A. V. Brandin,[31] D. Brown,[28] J. Bryslawskyj,[9] I. Bunzarov,[24] J. Butterworth,[42] H. Caines,[60] M. Calderón de la Barca Sánchez,[7] D. Cebra,[7] I. Chakaberia,[25,46] P. Chaloupka,[13] B. K. Chan,[8] F-H. Chang,[33] Z. Chang,[5] N. Chankova-Bunzarova,[24] A. Chatterjee,[57] S. Chattopadhyay,[57] J. H. Chen,[47] X. Chen,[45] X. Chen,[21] J. Cheng,[53] M. Cherney,[12] W. Christie,[5] G. Contin,[27] H. J. Crawford,[6] M. Csanad,[15] S. Das,[10] T. G. Dedovich,[24] I. M. Deppner,[18] A. A. Derevschikov,[39] L. Didenko,[5] C. Dilks,[38] X. Dong,[27] J. L. Drachenberg,[1] J. C. Dunlop,[5] L. G. Efimov,[24] N. Elsey,[59] J. Engelage,[6] G. Eppley,[42] R. Esha,[8] S. Esumi,[54] O. Evdokimov,[11] J. Ewigleben,[28] O. Eyser,[5] R. Fatemi,[26] S. Fazio,[5] P. Federic,[34] P. Federicova,[13] J. Fedorisin,[24] P. Filip,[24] E. Finch,[48] Y. Fisyak,[5] C. E. Flores,[7] L. Fulek,[2] C. A. Gagliardi,[51] T. Galatyuk,[14] F. Geurts,[42] A. Gibson,[56] D. Grosnick,[56] D. S. Gunarathne,[50] Y. Guo,[25] A. Gupta,[23] W. Guryn,[5] A. I. Hamad,[25] A. Hamed,[51] A. Harlenderova,[13] J. W. Harris,[60] L. He,[40] S. Heppelmann,[7] S. Heppelmann,[38] N. Herrmann,[18] A. Hirsch,[40] L. Holub,[13] Y. Hong,[27] S. Horvat,[60] B. Huang,[11] H. Z. Huang,[8] S. L. Huang,[49] T. Huang,[33] X. Huang,[53] T. J. Humanic,[35] P. Huo,[49] G. Igo,[8] W. W. Jacobs,[20] A. Jentsch,[52] J. Jia,[5,49] K. Jiang,[45] S. Jowzaee,[59] X. Ju,[45] E. G. Judd,[6] S. Kabana,[25] S. Kagamaster,[28] D. Kalinkin,[20] K. Kang,[53] D. Kapukchyan,[9] K. Kauder,[5] H. W. Ke,[5] D. Keane,[25] A. Kechechyan,[24] D. P. Kikoła,[58] C. Kim,[9] T. A. Kinghorn,[7] I. Kisel,[16] A. Kisiel,[58] L. Kochenda,[31] L. K. Kosarzewski,[58] A. F. Kraishan,[50] L. Kramarik,[13] L. Krauth,[9] P. Kravtsov,[31] K. Krueger,[4] N. Kulathunga,[19] L. Kumar,[37] R. Kunnawalkam Elayavalli,[59] J. Kvapil,[13] J. H. Kwasizur,[20] R. Lacey,[49] J. M. Landgraf,[5] J. Lauret,[5] A. Lebedev,[5] R. Lednicky,[24] J. H. Lee,[5] C. Li,[45] W. Li,[47] X. Li,[45] Y. Li,[53] Y. Liang,[25] J. Lidrych,[13] T. Lin,[51] A. Lipiec,[58] M. A. Lisa,[35] F. Liu,[10] H. Liu,[20] P. Liu,[49] P. Liu,[47] Y. Liu,[51] Z. Liu,[45] T. Ljubicic,[5] W. J. Llope,[59] M. Lomnitz,[27] R. S. Longacre,[5] S. Luo,[11] X. Luo,[10] G. L. Ma,[47] L. Ma,[17] R. Ma,[5] Y. G. Ma,[47] N. Magdy,[49] R. Majka,[60] D. Mallick,[32] S. Margetis,[25] C. Markert,[52] H. S. Matis,[27] O. Matonoha,[13] J. A. Mazer,[43] K. Meehan,[7] J. C. Mei,[46] N. G. Minaev,[39] S. Mioduszewski,[51] D. Mishra,[32] B. Mohanty,[32] M. M. Mondal,[22] I. Mooney,[59] D. A. Morozov,[39] Md. Nasim,[8] J. D. Negrete,[9] J. M. Nelson,[6] D. B. Nemes,[60] M. Nie,[47] G. Nigmatkulov,[31] T. Niida,[59] L. V. Nogach,[39] T. Nonaka,[10] G. Odyniec,[27] A. Ogawa,[5] K. Oh,[41] S. Oh,[60] V. A. Okorokov,[31] D. Olvitt, Jr.,[50] B. S. Page,[5] R. Pak,[5] Y. Panebratsev,[24] B. Pawlik,[36] H. Pei,[10] C. Perkins,[6] R. L. Pinter,[15] J. Pluta,[58] J. Porter,[27] M. Posik,[50] N. K. Pruthi,[37] M. Przybycien,[2] J. Putschke,[59] A. Quintero,[50] S. K. Radhakrishnan,[27] S. Ramachandran,[26] R. L. Ray,[52] R. Reed,[28] H. G. Ritter,[27] J. B. Roberts,[42] O. V. Rogachevskiy,[24] J. L. Romero,[7] L. Ruan,[5] J. Rusnak,[34] O. Rusnakova,[13] N. R. Sahoo,[51] P. K. Sahu,[22] S. Salur,[43] J. Sandweiss,[60] J. Schambach,[52] A. M. Schmah,[27] W. B. Schmidke,[5] N. Schmitz,[29] B. R. Schweid,[49] F. Seck,[14] J. Seger,[12] M. Sergeeva,[8] R. Seto,[9] P. Seyboth,[29] N. Shah,[47] E. Shahaliev,[24] P. V. Shanmuganathan,[28] M. Shao,[45] F. Shen,[46] W. Q. Shen,[47] S. S. Shi,[10] Q. Y. Shou,[47] E. P. Sichtermann,[27] S. Siejka,[58] R. Sikora,[2] M. Simko,[34] J. Singh,[37] S. Singha,[25] D. Smirnov,[5] N. Smirnov,[60] W. Solyst,[20] P. Sorensen,[5] H. M. Spinka,[4] B. Srivastava,[40] T. D. S. Stanislaus,[56] D. J. Stewart,[60] M. Strikhanov,[31] B. Stringfellow,[40] A. A. P. Suaide,[44] T. Sugiura,[54] M. Sumbera,[34] B. Summa,[38] X. M. Sun,[10] X. Sun,[10] Y. Sun,[45] B. Surrow,[50] D. N. Svirida,[3] P. Szymanski,[58] A. H. Tang,[5] Z. Tang,[45] A. Taranenko,[31] T. Tarnowsky,[30] J. H. Thomas,[27] A. R. Timmins,[19] D. Tlusty,[42] T. Todoroki,[5] M. Tokarev,[24] C. A. Tomkiel,[28] S. Trentalange,[8] R. E. Tribble,[51] P. Tribedy,[5] S. K. Tripathy,[22] O. D. Tsai,[8] B. Tu,[10] T. Ullrich,[5] D. G. Underwood,[4] I. Upsal,[5,46] G. Van Buren,[5] J. Vanek,[34] A. N. Vasiliev,[39] I. Vassiliev,[16] F. Videbæk,[5] S. Vokal,[24] S. A. Voloshin,[59] A. Vossen,[20] F. Wang,[40] G. Wang,[8] P. Wang,[45] Y. Wang,[10] Y. Wang,[53] J. C. Webb,[5] L. Wen,[8] G. D. Westfall,[30] H. Wieman,[27] S. W. Wissink,[20] R. Witt,[55] Y. Wu,[25] Z. G. Xiao,[53] G. Xie,[11] W. Xie,[40] J. Xu,[10] N. Xu,[27] Q. H. Xu,[46] Y. F. Xu,[47] Z. Xu,[5] C. Yang,[46] Q. Yang,[46] S. Yang,[5] Y. Yang,[33] Z. Ye,[11] Z. Ye,[11] L. Yi,[46] K. Yip,[5] I.-K. Yoo,[41] N. Yu,[10] H. Zbroszczyk,[58] W. Zha,[45] J. Zhang,[27] J. Zhang,[21] L. Zhang,[10] S. Zhang,[45] S. Zhang,[47] X. P. Zhang,[53] Y. Zhang,[45] Z. Zhang,[47] J. Zhao,[40] C. Zhong,[47] C. Zhou,[47] X. Zhu,[53] Z. Zhu,[46] and M. Zyzak[16]

(STAR Collaboration)

[1]*Abilene Christian University, Abilene, Texas 79699*
[2]*AGH University of Science and Technology, FPACS, Cracow 30-059, Poland*
[3]*Alikhanov Institute for Theoretical and Experimental Physics, Moscow 117218, Russia*

[4]*Argonne National Laboratory, Argonne, Illinois 60439*
[5]*Brookhaven National Laboratory, Upton, New York 11973*
[6]*University of California, Berkeley, California 94720*
[7]*University of California, Davis, California 95616*
[8]*University of California, Los Angeles, California 90095*
[9]*University of California, Riverside, California 92521*
[10]*Central China Normal University, Wuhan, Hubei 430079*
[11]*University of Illinois at Chicago, Chicago, Illinois 60607*
[12]*Creighton University, Omaha, Nebraska 68178*
[13]*Czech Technical University in Prague, FNSPE, Prague 115 19, Czech Republic*
[14]*Technische Universität Darmstadt, Darmstadt 64289, Germany*
[15]*Eötvös Loránd University, Budapest H-1117, Hungary*
[16]*Frankfurt Institute for Advanced Studies FIAS, Frankfurt 60438, Germany*
[17]*Fudan University, Shanghai 200433*
[18]*University of Heidelberg, Heidelberg 69120, Germany*
[19]*University of Houston, Houston, Texas 77204*
[20]*Indiana University, Bloomington, Indiana 47408*
[21]*Institute of Modern Physics, Chinese Academy of Sciences, Lanzhou, Gansu 730000*
[22]*Institute of Physics, Bhubaneswar 751005, India*
[23]*University of Jammu, Jammu 180001, India*
[24]*Joint Institute for Nuclear Research, Dubna 141 980, Russia*
[25]*Kent State University, Kent, Ohio 44242*
[26]*University of Kentucky, Lexington, Kentucky 40506-0055*
[27]*Lawrence Berkeley National Laboratory, Berkeley, California 94720*
[28]*Lehigh University, Bethlehem, Pennsylvania 18015*
[29]*Max-Planck-Institut für Physik, Munich 80805, Germany*
[30]*Michigan State University, East Lansing, Michigan 48824*
[31]*National Research Nuclear University MEPhI, Moscow 115409, Russia*
[32]*National Institute of Science Education and Research, HBNI, Jatni 752050, India*
[33]*National Cheng Kung University, Tainan 70101*
[34]*Nuclear Physics Institute AS CR, Prague 250 68, Czech Republic*
[35]*Ohio State University, Columbus, Ohio 43210*
[36]*Institute of Nuclear Physics PAN, Cracow 31-342, Poland*
[37]*Panjab University, Chandigarh 160014, India*
[38]*Pennsylvania State University, University Park, Pennsylvania 16802*
[39]*Institute of High Energy Physics, Protvino 142281, Russia*
[40]*Purdue University, West Lafayette, Indiana 47907*
[41]*Pusan National University, Pusan 46241, Korea*
[42]*Rice University, Houston, Texas 77251*
[43]*Rutgers University, Piscataway, New Jersey 08854*
[44]*Universidade de São Paulo, São Paulo 05314-970, Brazil*
[45]*University of Science and Technology of China, Hefei, Anhui 230026*
[46]*Shandong University, Qingdao, Shandong 266237*
[47]*Shanghai Institute of Applied Physics, Chinese Academy of Sciences, Shanghai 201800*
[48]*Southern Connecticut State University, New Haven, Connecticut 06515*
[49]*State University of New York, Stony Brook, New York 11794*
[50]*Temple University, Philadelphia, Pennsylvania 19122*
[51]*Texas A&M University, College Station, Texas 77843*
[52]*University of Texas, Austin, Texas 78712*
[53]*Tsinghua University, Beijing 100084*
[54]*University of Tsukuba, Tsukuba, Ibaraki 305-8571, Japan*
[55]*United States Naval Academy, Annapolis, Maryland 21402*
[56]*Valparaiso University, Valparaiso, Indiana 46383*
[57]*Variable Energy Cyclotron Centre, Kolkata 700064, India*
[58]*Warsaw University of Technology, Warsaw 00-661, Poland*
[59]*Wayne State University, Detroit, Michigan 48201*
[60]*Yale University, New Haven, Connecticut 06520*

(Received 24 August 2018; published 29 November 2018)

The transverse spin transfer from polarized protons to Λ and $\bar{\Lambda}$ hyperons is expected to provide sensitivity to the transversity distribution of the nucleon and to the transversely polarized fragmentation functions. We report the first measurement of the transverse spin transfer to Λ and $\bar{\Lambda}$ along the polarization direction of the fragmenting quark, D_{TT}, in transversely polarized proton-proton collisions at $\sqrt{s} = 200$ GeV with the STAR detector at RHIC. The data correspond to an integrated luminosity of 18 pb^{-1} and cover the pseudorapidity range $|\eta| < 1.2$ and transverse momenta p_{T} up to 8 GeV/c. The dependence on p_{T} and η are presented. The D_{TT} results are found to be comparable with a model prediction and are also consistent with zero within uncertainties.

DOI: 10.1103/PhysRevD.98.091103

The polarizations of Λ and $\bar{\Lambda}$ hyperons have been studied extensively in various aspects of spin effects in high energy reactions due to the self-spin-analyzing parity violating decay [1]. Many of them have been found to be quite surprising, for example, the induced transverse polarization with respect to the production plane in unpolarized hadron-hadron reactions [2] and the global polarization with respect to the reaction plane observed recently in heavy ion collisions [3]. On the other hand, Λ polarization transferred from polarized lepton or hadron beams (usually referred to as "spin transfer") in different reactions provides a natural connection to polarized fragmentation functions and the polarized parton densities of the nucleon. A number of measurements have been made in polarized lepton-nucleon deep inelastic scattering (DIS), for example, E665 [4], HERMES [5] and COMPASS [6], and in polarized hadron-hadron collisions in the STAR experiment at RHIC [7,8]. In particular, among the polarized parton distributions, the transversity distribution remains much less known than the helicity distribution due to its chiral-odd nature [9,10]. The transversity distribution describes the probability of finding a transversely polarized quark in a transversely polarized proton. Interestingly, the transverse spin transfer to Λ in lepton-hadron and/or hadron-hadron collisions provides a natural connection to transversity through polarized fragmentation functions [11–16]. Previously, sizable spin transfer along the normal direction of the Λ production plane, D_{NN}, was observed at large x_{F} with fixed target proton-proton collisions by the E704 Collaboration at Fermilab [17] and also in exclusive production in proton-proton reactions at low energy [18].

We report the first measurement of transverse spin transfer to Λ and $\bar{\Lambda}$ hyperons in transversely polarized proton-proton collisions at $\sqrt{s} = 200$ GeV with the STAR experiment at RHIC at Brookhaven National Laboratory. The transverse spin transfer, D_{TT}, to the Λ in proton-proton collisions is defined as

$$D_{\mathrm{TT}} \equiv \frac{d\sigma^{(p^{\uparrow}p\to\Lambda^{\uparrow}X)} - d\sigma^{(p^{\uparrow}p\to\Lambda^{\downarrow}X)}}{d\sigma^{(p^{\uparrow}p\to\Lambda^{\uparrow}X)} + d\sigma^{(p^{\uparrow}p\to\Lambda^{\downarrow}X)}} = \frac{d\delta\sigma^{\Lambda}}{d\sigma^{\Lambda}}, \qquad (1)$$

where $\uparrow$ ($\downarrow$) denotes the positive (negative) transverse polarization direction of the particles and $\delta\sigma^{\Lambda}$ is the transversely polarized cross section. Within the factorization framework, $\delta\sigma^{\Lambda}$ can be factorized into the convolution of parton transversity, polarized partonic cross section and the polarized fragmentation function [13]. As the $s(\bar{s})$ quark plays a dominant role in $\Lambda(\bar{\Lambda})$ hyperon's spin content, the measurements of D_{TT} for $\Lambda(\bar{\Lambda})$ hyperon provide a natural connection to the transversity distribution of strange and antistrange quarks [13,15,16]. Experimentally, the transverse spin transfer, D_{TT}, can be measured along the transverse polarization direction of the outgoing quark after the hard scattering.

The polarization of $\Lambda(\bar{\Lambda})$ hyperons, $P_{\Lambda(\bar{\Lambda})}$, can be measured from the angular distribution of the final state particles via their weak decay channel $\Lambda \to p\pi^{-}(\bar{\Lambda} \to \bar{p}\pi^{+})$,

$$\frac{dN}{d\cos\theta^{*}} \propto A(1 + \alpha_{\Lambda(\bar{\Lambda})}P_{\Lambda(\bar{\Lambda})}\cos\theta^{*}), \qquad (2)$$

where A is the detector acceptance varying with θ^{*} as well as other observables, $\alpha_{\Lambda(\bar{\Lambda})}$ is the weak decay parameter, and θ^{*} is the angle between the $\Lambda(\bar{\Lambda})$ polarization direction and the (anti-) proton momentum in the $\Lambda(\bar{\Lambda})$ rest frame. For the D_{TT} measurements in this analysis, the transverse polarization direction of the outgoing fragmenting parton is used to obtain θ^{*}. As there is a rotation along the normal direction of the scattering plane between the transverse polarization directions of incoming and outgoing quarks [19], the direction of the momentum of the outgoing parton is required, and the reconstructed jet axis adjacent to the $\Lambda(\bar{\Lambda})$ is used as the substitute for the direction of the outgoing fragmenting quark.

The data were collected at RHIC with the STAR experiment in the year 2012. An integrated luminosity of 18 pb^{-1} was sampled with transverse proton beam polarization. The proton polarization was measured for each beam and per fill using Coulomb nuclear interference (CNI) proton carbon polarimeters [20], which were calibrated using a polarized atomic hydrogen gas-jet target [21]. The average transverse polarizations for the two

TABLE I. Summary of selection cuts and the Λ and $\bar{\Lambda}$ candidate counts and the residual background fractions in each p_T bin. Here "DCA" denotes distance of closest approach, and $N(\sigma)$ quantitatively measures the distance of a particle track to a certain particle band in dE/dx versus rigidity space [26]. $\vec{l}$ is representative of the vector from the PV to the Λ decay point and $\vec{p}$ is the reconstructed momentum of Λ.

p_T[GeV/c]	(1,2)	(2,3)	(3,4)	(4,5)	(5,6)	(6,8)
N(hits) of daughter tracks	>14	>14	>14	>14	>14	>14
N(σ) dE/dx for daughters	<3	<3	<3	<3	<3	<3
DCA of daughter tracks [cm]	<0.80	<0.70	<0.60	<0.50	<0.45	<0.45
DCA of Λ ($\bar{\Lambda}$) to PV [cm]	<1.0	<1.0	<1.0	<1.0	<1.0	<1.0
cos ($\vec{l} \cdot \vec{p}$)	>0.995	>0.995	>0.995	>0.995	>0.995	>0.995
Decay Length [cm]	>3.5	>4.0	>4.0	>4.5	>5.0	>5.0
DCA of $p(\bar{p})$ to PV [cm]	>0.25	>0.20	>0.10	>0.05	>0.05	>0.05
DCA of $\pi^-(\pi^+)$ to PV [cm]	>0.60	>0.55	>0.50	>0.50	>0.50	>0.50
$\Lambda(\bar{\Lambda})$ counts	469681 (502226)	318358 (368042)	181550 (193221)	77866 (71833)	32441 (25571)	20256 (13486)
$\Lambda(\bar{\Lambda})$ bkg. frac.	0.065 (0.074)	0.079 (0.077)	0.071 (0.072)	0.065 (0.066)	0.070 (0.075)	0.084 (0.102)
Mass window(signal) [GeV/c^2]	(1.111, 1.119)	(1.111, 1.121)	(1.109, 1.123)	(1.108, 1.124)	(1.106, 1.126)	(1.104, 1.128)
Side-band (left) [GeV/c^2]	(1.090, 1.100)	(1.090, 1.100)	(1.088, 1.098)	(1.087, 1.097)	(1.085, 1.095)	(1.083, 1.093)
Side-band (right) [GeV/c^2]	(1.130, 1.140)	(1.132, 1.142)	(1.134, 1.144)	(1.135, 1.145)	(1.137, 1.147)	(1.139, 1.149)

beams were 58% and 64% for the analyzed data. Polarization up and down bunch patterns were changed between beam fills to minimize systematic uncertainties.

The primary detector subsystem used in this analysis is the time projection chamber (TPC) [22], which provides tracking for charged particles in the 0.5 T magnetic field in the pseudorapidity range of $|\eta| < 1.2$ with full azimuthal coverage. The measurement of specific energy loss, dE/dx, in the TPC gas provided information for particle identification. The barrel electromagnetic calorimeter (BEMC) [23] and endcap electromagnetic calorimeter (EEMC) [24] were used to generate the primary jet trigger information at STAR. The total BEMC coverage was $|\eta| < 1$ with full azimuth in 2012, and the EEMC extends the pseudorapidity coverage up to $\eta \sim 2$. The data samples used in this analysis were recorded with jet-patch (JP) trigger conditions which required a transverse energy deposit E_T in BEMC or EEMC patches (each covering a range of $\Delta\eta \times \Delta\phi = 1 \times 1$ in pseudorapidity and azimuthal angle) exceeding certain thresholds. The thresholds were $E_T \sim 3.5$ GeV for JP0, $E_T \sim 5.4$ GeV for JP1, or $E_T \sim 7.3$ GeV for JP2 or two adjacent jet patches (AJP) with each exceeding the threshold of $E_T \sim 3.5$ GeV for the AJP trigger.

The Λ and $\bar{\Lambda}$ candidates were reconstructed from their dominant weak decay channels, $\Lambda \to p\pi^-$ and $\bar{\Lambda} \to \bar{p}\pi^+$, with a branching ratio of 63.9% [25]. The location of the primary vertex (PV) was required to be within 60 cm of the center of the TPC along the beam axis to ensure uniform acceptance. The selection procedure of Λ and $\bar{\Lambda}$ candidates in this analysis is based on the topology of the weak decay using a method that is very similar to the one used in the previous longitudinal spin transfer measurement reported in Ref. [7]. (Anti-) proton and pion tracks were first identified based on dE/dx in the TPC. They were paired to form a $\Lambda(\bar{\Lambda})$ candidate, and topological selections were used to further reduce the background. The selection cuts were tuned in each hyperon p_T bin to keep the residual background fraction below 10%; these cuts are summarized in Table I.

As mentioned previously, reconstructed jets were employed to obtain the momentum direction of the fragmenting quark and thus the transverse polarization direction of hyperons for the D_{TT} measurement. In this analysis, jets were reconstructed using the anti-k_T algorithm [27] with a resolution parameter $R = 0.6$ and jet $p_T > 5$ GeV/c. In STAR, the TPC tracks and tower energies from the BEMC and EEMC are used for the jet reconstruction [28,29]. Then the association between $\Lambda(\bar{\Lambda})$ candidates and the adjacent reconstructed jet was made by constraining the radius, $\Delta R = \sqrt{(\Delta\eta)^2 + (\Delta\phi)^2}$, between the $\Lambda(\bar{\Lambda})$ momentum direction and the jet axis in $\eta - \phi$ space. The $\Lambda(\bar{\Lambda})$ candidates that have a jet with $\Delta R < 0.6$ were used in the following D_{TT} determination. The fraction of $\Lambda(\bar{\Lambda})$ candidates that have a matching jet increases from about 30 to 90% from the lowest hyperon p_T bin to the highest.

After topological selections and jet correlation, the invariant mass distributions for the Λ and $\bar{\Lambda}$ candidates with $1 < p_T < 8$ GeV/c and $|\eta| < 1.2$ are shown in Fig. 1.

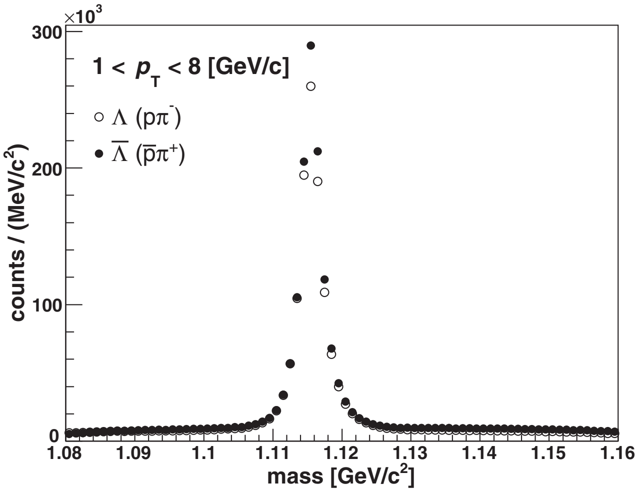

FIG. 1. Invariant mass distribution for Λ (open circles) and $\bar{\Lambda}$ (filled circles) candidates with $1 < p_{\mathrm{T}} < 8$ GeV$/c$ after selection in this analysis.

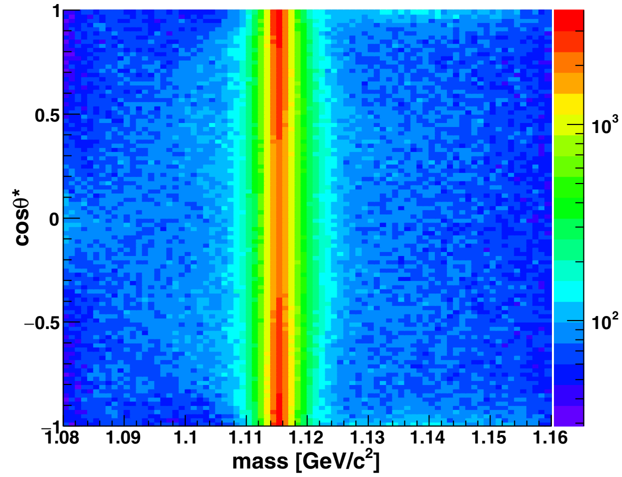

FIG. 2. Invariant mass distribution versus $\cos\theta^*$ for Λ candidates with $1 < p_{\mathrm{T}} < 8$ GeV$/c$ in this analysis as an example.

The values of the peak in the Λ and $\bar{\Lambda}$ mass distributions are in agreement with the PDG mass value $m_{\Lambda(\bar{\Lambda})} = 1.11568$ GeV$/c^2$ [25]. The two-dimensional distribution of invariant mass versus $\cos\theta^*$ as defined in Eq. (2) is shown in Fig. 2 for Λ candidates. A similar distribution was also obtained for $\bar{\Lambda}$ candidates. The bin counting method was used to obtain the raw yields of Λ and $\bar{\Lambda}$ candidates. The signal mass windows were chosen to be about 3σ of the mass width. These range from 1.111 to 1.119 GeV$/c^2$ in the lowest p_{T} bin to 1.104–1.128 GeV$/c^2$ in the highest p_{T} bin. About 1.02×10^6 Λ and 1.17×10^6 $\bar{\Lambda}$ candidates in the selected signal mass windows were kept as the signal. The residual background fractions were estimated by the side-band method and found to be 7–10%. The yields, background fractions and signal mass windows are listed in Table I. The $\bar{\Lambda}$ signal is larger than that of the Λ because of the effects of antiproton annihilation in the BEMC and EEMC, which provides additional energy to the JP trigger conditions for the $\bar{\Lambda}$.

The observed $\cos\theta^*$ spectra are affected by detector efficiency and acceptance as seen in Eq. (2). To minimize the systematics associated with acceptance and relative luminosity, D_{TT} has been extracted from the asymmetry in small $\cos\theta^*$ intervals using

$$D_{\mathrm{TT}} = \frac{1}{\alpha P_{\mathrm{beam}}\langle\cos\theta^*\rangle} \frac{\sqrt{N^{\uparrow}(\cos\theta^*)N^{\downarrow}(-\cos\theta^*)} - \sqrt{N^{\downarrow}(\cos\theta^*)N^{\uparrow}(-\cos\theta^*)}}{\sqrt{N^{\uparrow}(\cos\theta^*)N^{\downarrow}(-\cos\theta^*)} + \sqrt{N^{\downarrow}(\cos\theta^*)N^{\uparrow}(-\cos\theta^*)}}, \tag{3}$$

where $\alpha_{\Lambda} = 0.642 \pm 0.013$ [25], $\alpha_{\bar{\Lambda}} = -\alpha_{\Lambda}$, P_{beam} is the beam polarization and $\langle\cos\theta^*\rangle$ denotes the average value in the $\cos\theta^*$ interval. $N^{\uparrow(\downarrow)}$ is the Λ yield in the corresponding $\cos\theta^*$ bin when the proton beam is upward (downward) polarized. The relative luminosity between $N^{\uparrow}$ and $N^{\downarrow}$ is canceled in this cross-ratio asymmetry. The acceptance is also canceled as the acceptance in a small $\cos\theta^*$ interval is expected to remain the same when flipping the beam polarization [7], and the effect from limited $\cos\theta^*$ bin width is negligible. At RHIC both proton beams are polarized, and the single spin hyperon yield $N^{\uparrow(\downarrow)}$ was obtained by summing over the spin states of the other beam, as the beam fill patterns are nearly balanced with opposite polarizations.

The yields $N^{\uparrow}$ and $N^{\downarrow}$ were first determined in each $\cos\theta^*$ interval from the observed Λ or $\bar{\Lambda}$ candidate yields in the chosen mass interval, and the raw spin transfer, $D_{\mathrm{TT}}^{\mathrm{raw}}$, was extracted using Eq. (3) in each $\cos\theta^*$ bin. Then the $D_{\mathrm{TT}}^{\mathrm{raw}}$ values were averaged over the entire $\cos\theta^*$ range in each hyperon p_{T} bin. As single spin yields can be obtained with either beam polarized, we have two independent measurements for the same physics η range, but with different detector coverage, by treating one beam as polarized and summing over the polarization states of the other beam. After confirming their consistency, we determined the final $D_{\mathrm{TT}}^{\mathrm{raw}}$ results from the weighted mean.

Figure 3(a) shows the beam combined $D_{\mathrm{TT}}^{\mathrm{raw}}$ versus $\cos\theta^*$ for Λ hyperons in the positive and negative η regions, respectively, with $2 < p_{\mathrm{T}} < 3$ GeV$/c$ provided as an example. The results for $\bar{\Lambda}$ hyperon are shown in Fig. 3(b). Positive η is defined along the direction of the incident polarized beam. The extracted $D_{\mathrm{TT}}^{\mathrm{raw}}$ is constant

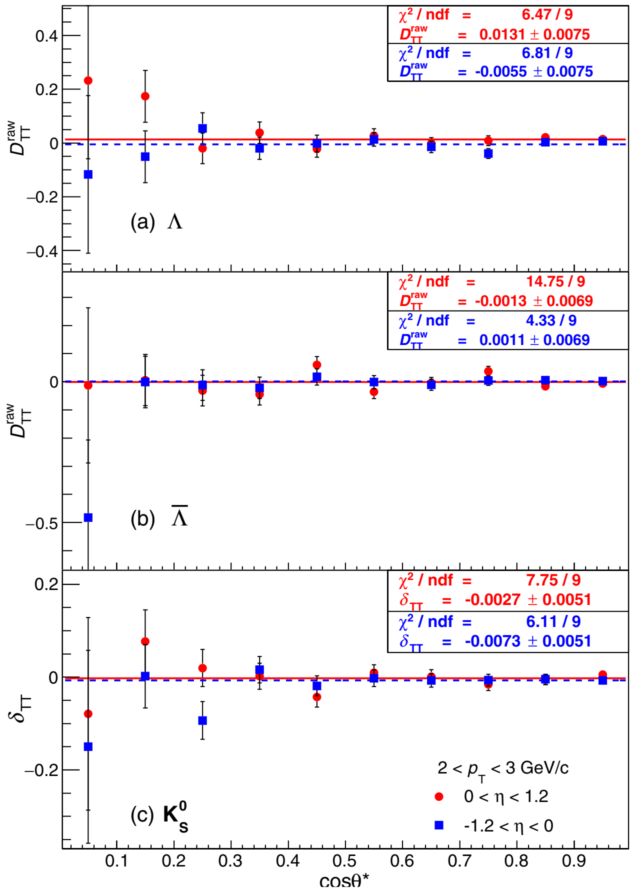

FIG. 3. Spin transfer D_{TT}^{raw} versus $\cos\theta^*$ for (a) Λ and (b) $\bar{\Lambda}$ hyperons, and (c) the spin asymmetry δ_{TT} for the control sample of K_S^0 mesons versus $\cos\theta^*$ in the p_T bin of $(2, 3)$ GeV$/c$. The red circles show the results for positive pseudorapidity η with respect to the polarized beam, and the blue squares show the results for negative η. Only statistical uncertainties are shown.

with $\cos\theta^*$ as expected and confirmed by the quality of the fit. A null measurement was performed with the spin transfer for the spinless K_S^0, δ_{TT}, as a cross check, which has a similar event topology. The δ_{TT} obtained with an artificial weak decay parameter $\alpha_{K_S^0} = 1$ is shown in Fig. 3(c). As expected, the results were found to be consistent with no spin transfer.

D_{TT}^{raw} values and their statistical uncertainties were then corrected for residual background dilution according to

$$D_{TT} = \frac{D_{TT}^{raw} - rD_{TT}^{bkg}}{1 - r}, \qquad (4)$$

$$\delta D_{TT} = \frac{\sqrt{(\delta D_{TT}^{raw})^2 + (r\delta D_{TT}^{bkg})^2}}{1 - r}, \qquad (5)$$

where r is the background fraction in each p_T bin estimated by the side-band method [8], and D_{TT}^{bkg} was obtained from the left and right side-band mass intervals as shown in last two rows of Table I using the same procedure as D_{TT}^{raw} following Eq. (3) and was consistent with zero within the statistical uncertainty.

The systematic uncertainties of D_{TT} include contributions from the decay parameter, α, from the measurement of the beam polarizations as well as uncertainty caused by the residual background fraction, event pile-up effects and trigger bias due to trigger conditions. The total systematic uncertainties in D_{TT} range from 0.0003 to 0.009 in different p_T bins, whereas the corresponding statistical uncertainties vary from 0.006 to 0.040. The above contributions are considered to be independent, and their sizes have been estimated as described below. The trigger bias is the dominant contribution to the systematic uncertainty.

The uncertainty in $\alpha_\Lambda = -\alpha_{\bar{\Lambda}} = 0.642 \pm 0.013$ corresponds to a 2% scale uncertainty in D_{TT}. The uncertainty in the RHIC beam polarization measurements contributes an additional 3.4% scale uncertainty in D_{TT}. The pile-up effect due to possible overlapping events recorded in the TPC was studied by examining the hyperon yield per event versus the STAR collision rate. A comparison between the yields per collision event found by fitting with a constant and a linear extrapolation to very low collision rates was used to estimate the pile-up contribution for different spin states, and the corresponding uncertainty to D_{TT} was found to be small (<0.005). The residual background fractions were estimated by the side-band method, and D_{TT} was corrected accordingly. The corresponding uncertainty was quantified from the difference in the results when the background fractions were estimated instead by fitting the mass spectra. This part is found to be also very small (<0.003). The data samples used in this analysis were recorded with jet-patch trigger conditions, which help to reach high transverse momenta of hyperons. However, these trigger conditions may bias the D_{TT} measurements by changing the natural composition of hyperon events with respect to the distributions of the hyperon momentum fraction in its associated jet, the hard production subprocesses, the flavor of the associated jet, the decay contribution, etc. The uncertainties caused by the above mentioned jet trigger conditions were studied with a Monte Carlo simulation of events generated using PYTHIA 6.4 [30] with the Perugia 2012 tune [31] and the STAR detector response package based on GEANT 3 [32]. The uncertainties from trigger bias were then estimated by comparing the D_{TT} values obtained from a theoretical model [16] before and after applying the trigger conditions. This yields uncertainties up to 0.008 with increasing p_T.

The STAR results for D_{TT} versus hyperon p_T are shown in Fig. 4 for Λ and $\bar{\Lambda}$ at both positive and negative η regions relative to the polarized beam in proton-proton collisions at $\sqrt{s} = 200$ GeV. About 60% of Λ or $\bar{\Lambda}$ are not primary particles but stem from decay of heavier hyperons. No corrections have been applied for decay contributions from heavier baryonic states. Several of the models do take into

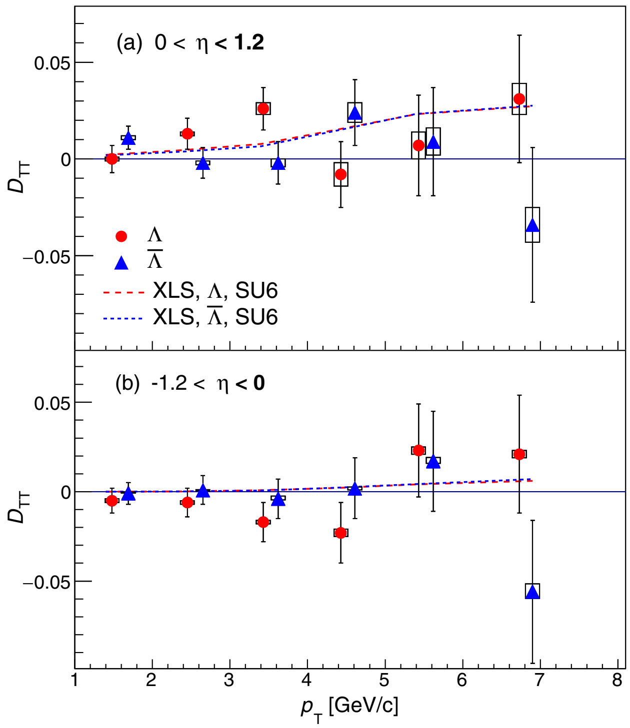

FIG. 4. Spin transfer D_{TT} for Λ and $\bar{\Lambda}$ versus p_T in polarized proton-proton collisions at $\sqrt{s} = 200$ GeV at STAR, in comparison with model predictions [15,16] for (a) positive η and (b) negative η. The vertical bars and hollow rectangles indicate the sizes of the statistical and systematic uncertainties, respectively. The $\bar{\Lambda}$ results have been offset to slightly larger p_T values for clarity.

account the decay contribution [13,15,16]. The statistical and systematic uncertainties are shown with vertical bars and open boxes, respectively. The systematic uncertainties in the positive η range are larger than those in the negative η range, owing to the larger trigger bias in the positive η range. These results provide the first measurements on transverse spin transfer of hyperons at a high energy of $\sqrt{s} = 200$ GeV. The D_{TT} results for Λ and $\bar{\Lambda}$ are consistent with zero within uncertainties. The data cover p_T up to 7 GeV/c, where $D_{TT} = 0.031 \pm 0.033(\text{stat}) \pm 0.008(\text{sys})$ for Λ and $D_{TT} = -0.034 \pm 0.040(\text{stat}) \pm 0.009(\text{sys})$ for $\bar{\Lambda}$ at $\langle\eta\rangle = 0.5$ and $\langle p_T\rangle = 6.7$ GeV/c. Strange quarks and antistrange quarks are expected to carry a significant part of the spins of Λ and $\bar{\Lambda}$; therefore, the measurements of transverse spin transfer to them can provide insights into the transversity distribution of strange quarks. Knowledge of transversity of valence quarks has been learned mostly from DIS experiments, but the transversity distribution of strange quarks is not yet constrained experimentally [33–35].

A few model predictions exist of hyperon transverse spin transfer in hadron-hadron collisions, based on different assumptions on the transversity distribution and transversely polarized fragmentation functions [13,15,16]. In Fig. 4, the D_{TT} data are compared with a model estimation calculated at $\langle\eta\rangle = \pm 0.5$, which is available for RHIC energy, with simple assumptions of the transversity (using the DSSV helicity distribution as input) and the $SU6$ picture of fragmentation functions [15,16]. The data are, in general, consistent with the model predictions. The D_{TT} of Λ and $\bar{\Lambda}$ are not in disagreement with each other, with a χ^2/ndf of 9.5/6. A possible difference between them could come, for example, from different fragmentation contributions from the nonstrange quarks.

In summary, we report the first measurement of the transverse spin transfer, D_{TT}, to Λ and $\bar{\Lambda}$ in transversely polarized proton-proton collisions at $\sqrt{s} = 200$ GeV at RHIC. The data correspond to an integrated luminosity of 18 pb^{-1} taken by the STAR experiment in 2012 and cover midrapidity, $|\eta| < 1.2$, and p_T up to 8 GeV/c. The D_{TT} value and precision in the highest p_T bin, where the effects are expected to be largest, are found to be $D_{TT} = 0.031 \pm 0.033(\text{stat}) \pm 0.008(\text{sys})$ for Λ and $D_{TT} = -0.034 \pm 0.040(\text{stat}) \pm 0.009(\text{sys})$ for $\bar{\Lambda}$ at $\langle\eta\rangle = 0.5$ and $\langle p_T\rangle = 6.7$ GeV/c. The results for D_{TT} are found to be consistent with zero for Λ and $\bar{\Lambda}$ within uncertainties and are also consistent with model predictions.

ACKNOWLEDGMENTS

We thank the RHIC Operations Group and RCF at BNL, the NERSC Center at LBNL, and the Open Science Grid consortium for providing resources and support. This work was supported in part by the Office of Nuclear Physics within the U.S. DOE Office of Science, the U.S. National Science Foundation, the Ministry of Education and Science of the Russian Federation, Natural Science Foundation of China, Chinese Academy of Science, the Ministry of Science and Technology of China, the Major State Basic Research Development Program in China (No. 2014CB845406) and the Chinese Ministry of Education, the National Research Foundation of Korea, Czech Science Foundation and Ministry of Education, Youth and Sports of the Czech Republic, Department of Atomic Energy and Department of Science and Technology of the Government of India, the National Science Centre of Poland, the Ministry of Science, Education and Sports of the Republic of Croatia, RosAtom of Russia and German Bundesministerium fur Bildung, Wissenschaft, Forschung and Technologie (BMBF) and the Helmholtz Association.

[1] T. D. Lee and C. N. Yang, Phys. Rev. **108**, 1645 (1957).
[2] G. Bunce *et al.*, Phys. Rev. Lett. **36**, 1113 (1976).
[3] L. Adamczyk *et al.* (STAR Collaboration), Nature (London) **548**, 62 (2017).
[4] M. R. Adams *et al.* (E665 Collaboration), Eur. Phys. J. C **17**, 263 (2000).
[5] A. Airapetian *et al.* (HERMES Collaboration), Phys. Rev. D **74**, 072004 (2006).
[6] M. Alekseev *et al.* (COMPASS Collaboration), Eur. Phys. J. C **64**, 171 (2009).
[7] B. I. Abelev *et al.* (STAR Collaboration), Phys. Rev. D **80**, 111102 (2009).
[8] J. Adam *et al.* (STAR Collaboration), arXiv:1808.07634.
[9] V. Barone, A. Drago, and P. G. Ratcliffe, Phys. Rep. **359**, 1 (2002).
[10] M. Grosse Perdekamp and F. Yuan, Annu. Rev. Nucl. Part. Sci. **65**, 429 (2015).
[11] X. Artru and M. Mekhfi, Nucl. Phys. **A532**, 351 (1991).
[12] R. L. Jaffe, Phys. Rev. D **54**, R6581 (1996).
[13] D. de Florian, J. Soffer, M. Stratmann, and W. Vogelsang, Phys. Lett. B **439**, 176 (1998).
[14] B. Q. Ma, I. Schmidt, J. Soffer, and J. J. Yang, Phys. Rev. D **64**, 014017 (2001).
[15] Q. H. Xu and Z. T. Liang, Phys. Rev. D **70**, 034015 (2004).
[16] Q. H. Xu, Z. T. Liang, and E. Sichtermann, Phys. Rev. D **73**, 077503 (2006).
[17] A. Bravar *et al.* (E704 Collaboration), Phys. Rev. Lett. **78**, 4003 (1997).
[18] F. Balestra *et al.* (DISTO Collaboration), Phys. Rev. Lett. **83**, 1534 (1999).
[19] J. C. Collins, S. F. Heppelmann, and G. A. Ladinsky, Nucl. Phys. **B420**, 565 (1994).
[20] H. Okada *et al.*, Phys. Lett. B **638**, 450 (2006).
[21] O. Jinnouchi *et al.*, *Proceedings of the 16th International Spin Physics Symposium, SPIN2004*, (World Scientific, Singapore, 2004), p. 515.
[22] M. Anderson *et al.* (STAR Collaboration), Nucl. Instrum. Methods A **499**, 659 (2003).
[23] M. Beddo *et al.* (STAR Collaboration), Nucl. Instrum. Methods A **499**, 725 (2003).
[24] C. E. Allgower *et al.* (STAR Collaboration), Nucl. Instrum. Methods A **499**, 740 (2003).
[25] M. Tanabashi *et al.* (Particle Data Group), Phys. Rev. D **98**, 030001 (2018).
[26] B. I. Abelev *et al.* (STAR Collaboration), Phys. Rev. C **75**, 064901 (2007).
[27] M. Cacciari, G. P. Salam, and G. Soyez, J. High Energy Phys. 04 (2008) 063.
[28] L. Adamczyk *et al.* (STAR Collaboration), Phys. Rev. Lett. **115**, 092002 (2015).
[29] L. Adamczyk *et al.* (STAR Collaboration), Phys. Rev. D **95**, 071103 (2017).
[30] T. Sjostrand, S. Mrenna, and P. Z. Skands, J. High Energy Phys. 05 (2006) 026.
[31] P. Z. Skands, Phys. Rev. D **82**, 074018 (2010).
[32] R. Brun *et al.*, CERN, Report No. CERN-DD-EE-84-1, 1987.
[33] M. Anselmino, M. Boglione, U. D'Alesio, S. Melis, F. Murgia, and A. Prokudin, Phys. Rev. D **87**, 094019 (2013).
[34] Z. B. Kang, A. Prokudin, P. Sun, and F. Yuan, Phys. Rev. D **93**, 014009 (2016).
[35] M. Radici and A. Bacchetta, Phys. Rev. Lett. **120**, 192001 (2018).